J Mater Sci (2008) 43:4789–4800
DOI 10.1007/s10853-008-2676-0

Accelerated creep testing for aramid fibres using the stepped isothermal method

K. G. N. C. Alwis · C. J. Burgoyne

Received: 29 December 2006 / Accepted: 24 April 2008 / Published online: 24 May 2008

Abstract The article shows how the stepped isothermal method (SIM), which has hitherto been applied to polyester fibres, can be applied to the creep testing of aramids. The method is an improvement over the time temperature superposition method since a complete creep curve can be obtained from a single fibre. However, adjustments have to be made to account for the temperature changes and the past history of the fibre. Techniques are shown for performing these adjustments and the resulting master curves are compared from several different tests with different temperature sequences. Activation energies are calculated, which show that the same mechanism is acting at all stages, and creep rupture lifetime predictions are made which are longer than those hitherto made by extrapolations from short-term creep tests.

Introduction

The use of aramid fibres for applications where permanent high stresses are expected (e.g., as prestressing tendons in concrete, or stay cables in bridges) is hampered by the lack of adequate long-term creep and stress-rupture models. The reliability of life prediction models could be improved if stress-rupture data were available at low stress levels, but this is difficult and expensive to obtain using conventional creep tests because of the long time needed to reach failure. However, creep of aramids is a thermally activated process so it is possible to accelerate the process to obtain failure within a few hours. This article reports work to investigate the application of the stepped isothermal method (SIM) to aramid fibres. In SIM testing a single yarn specimen is tested at a specific stress level under a series of increasing temperature steps; a single response curve, known as the master curve, is then obtained which predicts the long-term behaviour. Some manipulation of the data is required in order to compensate for the temperature steps, but the technique has many advantages over the time temperature superposition principle (TTSP) or conventional creep testing, and it can be automated to obtain long-term stress-rupture data points relatively easily. The SIM method seems promising as it shows repeatability when a number of tests are carried out and it is proposed as a reliable method to generate rupture data at low stress levels.

Thornton et al. [1–3] first applied the SIM to predict the long-term creep behaviour of geogrids in soil reinforcement applications, for which there are now standards [4]; an application of the method has been described by Zornberg et al. [5]. The principle of the SIM is that a single element (in this case a yarn) is placed in a testing machine and loaded to a chosen force. The temperature is then raised in steps (typically by a few degrees centigrade) and kept constant in each step for a fixed period of time (typically a few hours); some manipulation of the data is required in order to compensate for the temperature steps. The claimed advantage for the method is that a single specimen can be used, which reduces the handling effects, and the complete creep/time behaviour can be obtained from one specimen. Although the method itself is not new, it is not believed that it has hitherto been applied to high-modulus fibres like aramids whose molecular structure differs significantly from the materials used in geotechnical applications.

K. G. N. C. Alwis
WS Atkins, Surrey, UK

C. J. Burgoyne (✉)
Department of Engineering, University of Cambridge,
Trumpington St., Cambridge CB2 1PZ, UK
e-mail: cjb@eng.cam.ac.uk

SIM can be considered as a special case of the TTSP, a detailed description of which is given elsewhere [6–8]. In SIM tests, a single specimen is tested at a sequence of temperature levels under a constant load, whereas in TTSP testing different specimens are tested at each temperature level. SIM is very promising when compared to TTSP and conventional creep tests since a yarn can be tested until it fails in a much shorter time scale, which depends on the temperature and time steps adopted. Stress-rupture points can also be determined as an end product of the creep master curve, as can the activation energy of the creep process.

The analysis of SIM data differs from that during TTSP; three different adjustments are needed for each SIM test to produce a single master creep curve. With time plotted horizontally, and strain plotted vertically, the *vertical shift* allows for the strains caused by the change in temperature, taking account of the creep that occurs while the temperature change is taking place. *Rescaling* is needed to allow for the previous history of the specimen; when the temperature changes some allowance must be made for the fact that some creep has already taken place under the previous time steps, unlike TTSP when each test is separate. This adjustment takes the form of a shift in the time direction when plotted against a *linear* time scale. The *horizontal shift* takes the form of a shift on a creep strain versus log (time) plot and is similar to the technique used in TTSP to allow comparison of tests at different temperatures [8].

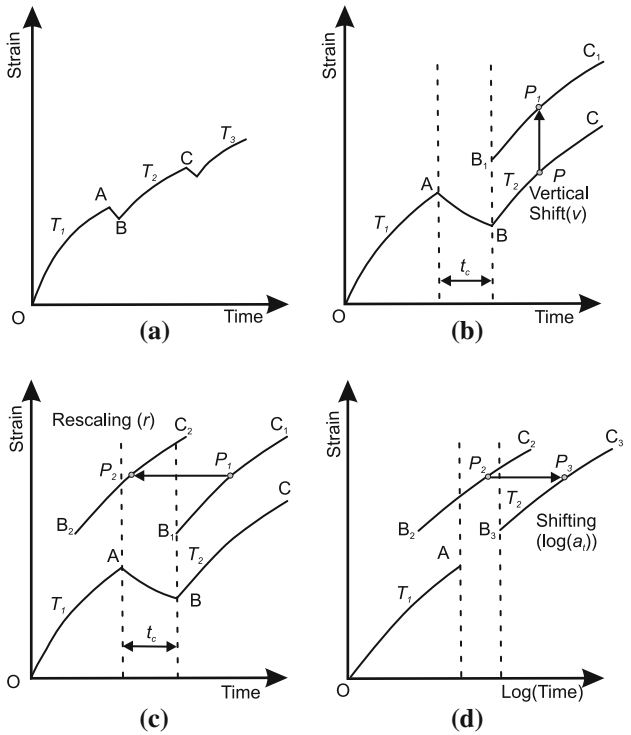

Fig. 1 Schematic SIM procedure: (**a**) measured data, (**b**) strain adjustment, (**c**) rescaling, and (**d**) shifting

Each of these adjustments is described schematically in Fig. 1. The stress-rupture prediction comes from the end of the master curve when the specimen fails under a specific load and temperature.

Several researchers have investigated the temperature dependence of the horizontal shift factor and proposed various empirical formulas. In particular, the WLF equation (Williams–Landel–Ferry) is often used [9], but it is restricted to materials above the glass transition temperature. Since aramid fibres do not display a glass transition, but remain crystalline at all temperatures, the relationship between the temperature and the horizontal shift factor, $\log(a_t)$, is instead based on the Arrhenius equation, which assumes that creep is a thermally activated process and will obey the kinetic rate theory. The time taken to failure is thus given by:

$$t_i = B \exp^{[\Delta H/RT]} \tag{1}$$

where ΔH is the activation energy, R the universal gas constant, and T is the absolute temperature.

This leads to the following relationship [10]:

$$\log(a_t) = \frac{\Delta H}{2.30R}\left(\frac{1}{T} - \frac{1}{T_R}\right) \tag{2}$$

The superposition theory is only valid if the same mechanism is present at all the temperature levels; this can be checked by determining the activation energy of the process, which should be independent of temperature.

To have any validity, all master curves produced by SIM at different time and temperature steps should overlap and must give consistent rupture times with acceptable accuracy. To accomplish this a suitable test procedure was planned to cover many time and temperature step sequences.

Materials and experimental set-up

The purpose of this study was to determine whether the method could be applied to aramid fibres, so at the outset only one type of fibre (Kevlar-49) was tested. In subsequent work the procedure is being extended to other high-modulus fibres. In the sample tests described here, Kevlar-49 yarns were used, with an average breaking strength (ABL), obtained from 12 short-term tests, of 445 N. The cross-sectional area of the yarn was 0.1685×10^{-6} m^2. All subsequent stress levels will be expressed as a percentage of this ABL.

The tensile tests were carried out in a conventional testing machine, using round bar clamps that have also been used for long-term dead-weight testing of yarns. The testing set-up is shown in Fig. 2. The oven was set up within the test machine, with the two clamps mounted on

Fig. 2 Test set-up showing oven installed in test machine

extension pieces so that the complete test specimen lies inside the oven. The load was applied by moving the cross-head of the machine at a specific rate (5 mm/min); the cross-head movement and the load level were recorded.

All tests started at 25 °C as it was easy to control this temperature by heating only. The testing machine was kept in a temperature-controlled room where the temperature was maintained at 21 °C. It was not possible to carry out any tests below this value since the oven had no cooling facility.

It is essential to know accurately the strain of the specimen just after the initial loading in order to compare the creep curves at different temperatures. A small error here results in displacing the creep curves on the creep strain axis, which then makes it impossible to obtain smooth master curves by making only time shifts. A detailed analysis has been carried out using the raw data (cross-head movement of the machine and load level) to determine the absolute zero of the stress–strain curve of a yarn specimen, which then enables the accurate strain immediately after loading to be determined [7]. The technique is described briefly here for completeness.

Jaw adjustment

An error is associated with the clamping system due to initial slack and lack of a well-defined point of load transfer around the jaws, which means that the cross-head movement of the testing machine does not represent the accurate change of length of a yarn for a given load. This "jaw effect" means that the effective gauge length is not the same as the nominal gauge length. The accurate effective length is therefore defined as the addition of the nominal gauge length and the jaw effect.

The secant modulus of the yarns varies with load level. It can be expressed in terms of measurable quantities and the unknown amount of slack and jaw effect:

$$E_j = \frac{\text{stress}}{\text{strain}} = \frac{P_{ij}(l_{gi} + l_{jawi})}{A(e_{ij} - s_i)} \tag{3}$$

where i is the specimen number, j the loading level, E_j the secant modulus, P_{ij} the load, A the cross-sectional area of the yarn, s_i the initial slack, e_{ij} the cross-head movement, l_g the nominal gauge length, and l_{jaw} is the jaw effect.

There will also be experimental error in the determination of the extension, a_{ij}, which varies from reading to reading. Re-arranging Eq. 3:

$$e_{ij} = \frac{P_{ij}(l_{gi} + l_{jawi})}{AE_j} + s_i + a_{ij} \tag{4}$$

There are three unknowns: the jaw effect and the amount of slack should be constant for any given test, while the secant modulus should be the same for all tests at the same load level. The error term has a different value for each reading. To determine the jaw effect, the amount of slack and the secant modulus, the error in Eq. 4 was minimised using a built-in routine in Matlab. It was found that the jaw effect does not vary with the loading level or with the nominal gauge length but is constant for a given machine and specimen combination [7]. Once the jaw effect and initial slackness have been determined, it is possible to determine the accurate stress versus strain curve.

A similar procedure can be easily carried out to determine the stress versus strain curves for a sequence of temperature levels (Fig. 3). This figure can be used to determine the initial strains for a given stress level at different temperatures. For example, points at which the dashed line crosses the stress–strain curves are the initial strain values at 70% ABL. Only the stress–strain curve at 25 °C will be used in SIM tests since all tests start at that temperature.

Testing procedure

A series of SIM tests were carried out at 70% ABL on Kevlar-49 with different temperature steps and with different durations for each step.

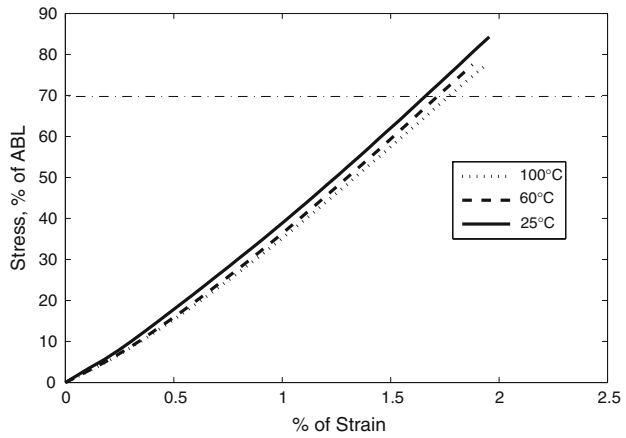

Fig. 3 Accurate stress–strain curves

Table 1 SIM tests at different temperature steps (°C) at 70% ABL

Test no.	No. of tests	Time duration for each temperature step (h)				
		5	5	5	5	5
SIM70-01	2	25	40	60	80	100[a]
SIM70-02	2	25	40	80	100[a]	–
SIM70-03	2	25	40	60	100[a]	–
SIM70-04	2	25	40	60	80	120[a]
SIM70-05	2	25	40	80	120[a]	–
SIM70-06	2	25	60	80	100[a]	–
SIM70-07	2	25	60	100[a]	–	–
SIM70-08	2	25	60	80	120[a]	–

[a] Final step extended until failure

Table 2 SIM tests at different temperature steps (°C) at 50% ABL

Test no.	No. of tests	Time duration for each temperature step (h)				
		5	5	5	5	5
SIM50-01	2	25	60	100	120	160[a]
SIM50-02	2	25	80	100	120	160[a]
SIM50-03	2	25	60	120	160[a]	–
SIM50-04	1	25	60	100	140	–
SIM50-05	1	25	60	100	120	140
SIM50-06	2	25	80	120	160[a]	–
SIM50-07	1	25	80	100	140	–
SIM50-08	1	25	80	100	120	140
SIM50-09	1	25	60	120	140	–
SIM50-10	1	25	80	120	140	–

[a] Final step extended until failure

Load was applied only after the temperature had reached 25 °C, so no initial correction for temperature was needed. Tables 1 and 2 show the temperature sequences used for the tests reported here; different sequences were used since, if the method is to be valid, similar master curves must be obtained no matter what temperature steps are used.

Each yarn was tested to failure; the failure point could be observed from the load reading of the testing machine and it was not necessary to open the oven for investigation. Each test was repeated twice, with the following nomenclature:

- SIM70-01-01
- SIM70-01-02

'70' denotes the load level, the succeeding number '01' denotes the temperature sequence (as in Tables 1 and 2) and the last number denotes the repetition of the test.

Description of the SIM method

The actual testing procedure is straightforward; the complication of SIM testing lies in the adjustments that have to be performed.

Adjustment of strain for change in temperature—the vertical shift

An adjustment has to be made for the change in length of the yarn due to the temperature change, and also for the creep that occurs in the short period while the temperature change is taking place.

Figure 4 shows a schematic picture of a temperature step. The temperature is raised from T_1 to T_2 over the time, t_c. Point B represents the creep strain just after the temperature step; B′ is the strain that would have been observed due to thermal contraction alone (aramid fibres have a negative coefficient of axial thermal expansion). However, the final creep strain, B, is observed due to continuing creep over time, t_c (B′B). The adjusted strain just after the temperature step ($\overline{\mathrm{B}}$) can be found by two methods:

(a) by adding the thermal contraction, so $\overline{\mathrm{B}} = \mathrm{B} + \mathrm{B}'\mathrm{B}''$, or
(b) by adding the creep over t_c, so $\overline{\mathrm{B}} = \mathrm{B}'' + \mathrm{B}'\mathrm{B}$

To calculate the distance B′B″, an accurate value of the coefficient of axial thermal expansion (CTE) is needed, but in the literature different values are stated (Table 3). Various values have been observed under different testing conditions. For example, Guimaraes [11] stated that the CTE was strain dependent, but he had carried out tests on Kevlar-49 in an aqueous environment. Pottick et al. [12], Ii et al. [13] and Rojstaczer et al. [14] quoted different values for the CTE but all tests were carried out at low stress levels. The difference of the values of CTE may be attributed to various factors such as dimensional variations of the clamp system, temperature gradient along the specimen, whether the specimen (yarn) was twisted or not and whether the tests were being carried out in air or in aqueous solutions.

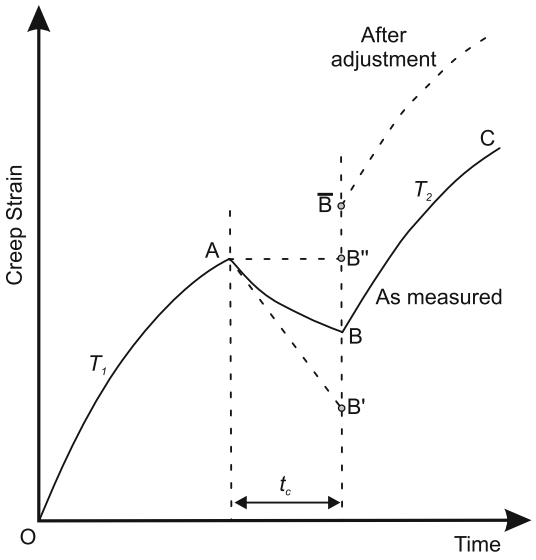

Fig. 4 Vertical adjustment at one temperature step

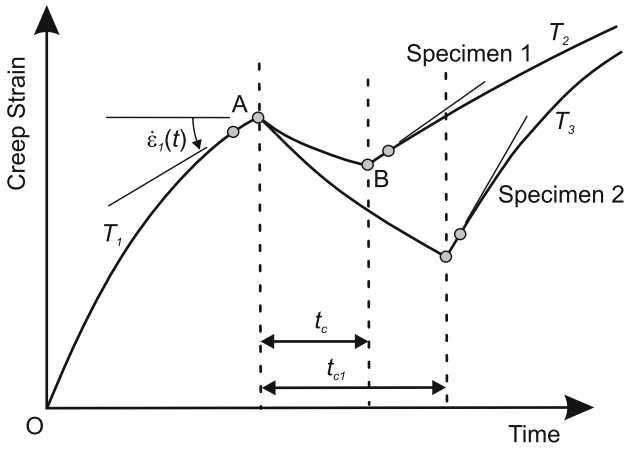

Fig. 5 Measurements of creep rate before and after temperature step

In the present analysis, tests were carried out at two load levels (50 and 70% ABL) at temperatures ranging from 25 to 160 °C. None of the past data on CTE were based on these limits and it was not possible to use the CTE values to calculate the thermal adjustment ($B'B''$), since accurate vertical adjustments were needed to make smooth master curves. A separate series of thermal experiments would be needed which was beyond the scope of the present study. Thus, method (a) was not considered to be suitable.

In contrast, method (b) can be performed using measured values, but at the cost of carrying out additional tests. Changes of the creep rate over time t_c can be found by conducting separate creep tests over the time step from temperature T_1 to a variety of higher temperatures. Creep gradients just before and just after the temperature step can be calculated by considering two close points on the creep strain curve. As an example, consider Fig. 5, which shows two specimens. They are held at a constant temperature T_1 up to point A; $\dot{\varepsilon}_1(t)$ is the creep gradient just before the temperature step. One specimen is then heated to temperature T_2, while the other takes longer to reach a higher temperature T_3. The creep gradients just after the temperature step can then be determined. Because the rate of heating of the oven is kept constant, the creep rates measured in these tests *after* the temperature step can be assumed to be the same as the creep rates *during* the temperature steps in the SIM specimens.

A pilot test was carried out to check the variation of the creep gradients with temperature. In that test four different temperature levels were used for the higher temperature after the step (Fig. 6). A quadratic variation of the creep gradients with the temperature was observed:

$$\dot{\varepsilon}(t) = \beta_0(T - \beta_1)^2 \tag{5}$$

The coefficients β_0, β_1 can be determined by a non-linear least square method.

In this testing, the maximum oven capacity of 5 °C/min (300 °C/h) was used for all temperature steps, so:

$$T = T_1 + 300 \times (t - t_1) \tag{6}$$

where T is the temperature, T_1 the initial temperature just before a desired step, t the time measured from the start of the experiment (hours), and t_1 is the time just before the temperature step (hours).

The total creep over time, $t_c(BB')$ can then be found by integration:

Table 3 Published data on the CTE of Kevlar-49

	Pottick et al. [12]	Ii et al. [13]	Rojstaczer et al. [14]	Guimaraes [11]
Specimen length (cm)	Yarn 30	Yarn 17	Fibres 1–2.5	Yarns 50
Temperature rate (°C/min)	5	7.5	1	0.66
Temperature range (°C)	20–200	−100–360	20–340	5–75
Applied stress (MPa)	60–130	50	220	50–1200
CTE ($\times 10^{-6}$/°C)	−3.2	−6.7	−5.7 (for $T < 80$ °C)	−3.9 to − 8.0
Testing medium	Air	Air	Air	Distilled water

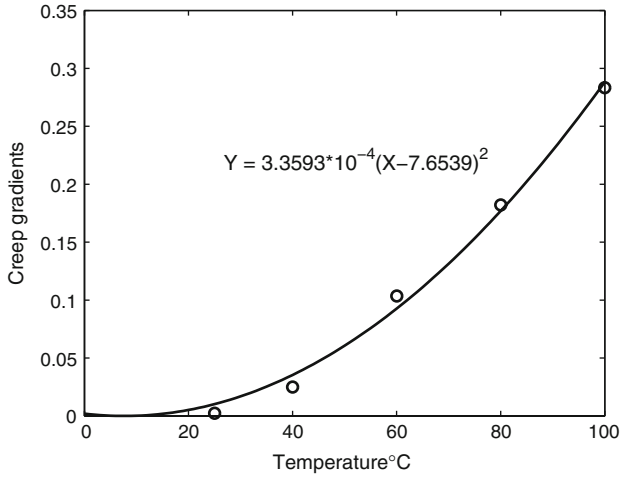

Fig. 6 Creep rates against temperature after temperature step

$$\mathrm{BB}' = \int_{t_1}^{t_2} \int_{T_1}^{T_2} \left[\beta_0 (T - \beta_1)^2\right] \mathrm{d}T \, \mathrm{d}t \tag{7}$$

Substituting Eq. 6 in Eq. 7 and letting $t_2 - t_1 = t_c$:

$$\mathrm{BB}' = \beta_0 \left\{ \left(T_1^2 + \beta_1^2 - 2T_1\beta_1\right) t_c + 300(T_1 - \beta_1) t_c^2 + 3 \times 10^4 t_c^3 \right\} \tag{8}$$

Equation 8 is independent of the CTE and can be used to calculate the vertical adjustment, which will account for the thermal contraction and the creep of the yarn over the temperature step. A similar procedure was used at each temperature step in all SIM master curves to find the adjusted value, $\overline{\mathrm{B}}$.

Based on these results it was decided to have a minimum of two supplementary creep tests at a jump to determine the non-linear variation of the creep gradients with temperature. This may seem a disadvantage of the method, but if SIM were to be used for a large scale testing programme, these test extra tests would only need to be carried out once.

Rescaling procedure

Rescaling is unique to SIM and accounts for the thermal history of the specimen. One of the main differences with the SIM approach is that the history of the specimen at different temperatures is not the same as in TTSP, where each specimen is subjected to a certain temperature level starting from room temperature. In SIM testing the specimen has a temperature history.

The following assumptions are made in the SIM technique:

- The temperature step only changes the rate of creep, not the mechanism.
- Recovery of creep does not occur while the temperature step takes place.

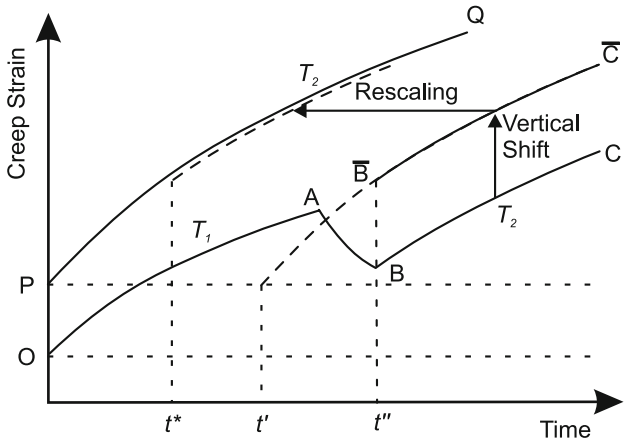

Fig. 7 Rescaling procedure

- The Boltzman superposition principle can be used to model the entire creep strain behaviour over the temperature range. The temperature step is assumed to accelerate the creep rate.
- The states at both the lower and the higher temperatures are stable and would be readily achievable under the TTSP approach.

Figure 7 shows the strain response for two temperature steps. The curve OABC is the measured response of the SIM specimen through the first two temperature steps. OA$\overline{\mathrm{BC}}$ is the response after making the vertical strain adjustment. PQ is the response of a TTSP test carried out at the higher temperature T_2. It is necessary to determine the time t' which represents the notional starting time for a TTSP specimen that would have the same response as the SIM specimen at the higher temperature. The value $t'' - t'$ is assumed to be the time needed for a specimen, which had been at T_2, to arrive at the creep state at time t''. It should be equal to t^* from the TTSP curve. The selection of t' for each temperature step has a great influence when obtaining smooth master curves. A graphical method is used to obtain an initial estimate of the time t' which is then refined numerically.

Numerical procedure to generate smooth master curves

A numerical procedure has been developed to select the rescaling time t' (which is applied in *linear* time) and the time shifting parameter $\log(a_t)$ (which is applied in logarithmic time, as in a conventional TTSP analysis), to produce a smooth master curve. Both rescaling and shifting factors are considered together to produce a smooth curve at a temperature step.

To describe the technique a single temperature step has been considered (Fig. 1). The main objective is to obtain a smooth curve at the overlapping region of two curve segments, which correspond to different temperature levels.

The creep curve segment that belongs to the higher temperature level (BC) is adjusted for the vertical shift, rescaled in *linear* time scale and shifted along the logarithmic time axis to produce a smooth master curve.

Step 1: An arbitrary point, P, on line BC is considered:

$$P \equiv [t_i,\ \varepsilon_i] \tag{9}$$

where i represents each data point.

Step 2: After the vertical strain adjustment (v_j), the line BC is moved to a new position B_1C_1 (Fig. 1b). The vertical strain adjustment, v_j, is similar to the value $B'' + B'B$ as described above. Point P moves to a new position P_1:

$$P \equiv \left[t_i,\ (\varepsilon_i + v_j)\right] \tag{10}$$

where j represents each adjustment.

Step 3: After the rescaling in *linear* time (by r_j, in hours) to account for the thermal history, the line B_1C_1 is moved to a position B_2C_2 (Fig. 1c):

$$P_2 \equiv \left[(t_i - r_j), (\varepsilon_i + v_j)\right] \tag{11}$$

Step 4: Finally, the shifting is carried out on a logarithmic time axis and the line B_2C_2 is moved to a new position B_3C_3 by an amount of $\log(a_t)$ (Fig. 1d):

$$P_3 \equiv \left[\log(t_i - r_j) + \log(a_t),\ (\varepsilon_i + v_j)\right] \tag{12}$$

Equation 12 contains two unknowns: r_j and $\log(a_t)$. Their optimal values are obtained by fitting a polynomial through the data on either side of the step, and then calculating the sum of square errors (SSE) for different values of the rescaling factor r_j and shift factor $\log(a_t)$.

The degree of the polynomial used for the smooth matching had to be fixed, as did the time interval on each side of the gap AB_3. A pilot study showed that no advantage was obtained by using a polynomial of higher order than three because of over-fitting, and the time interval used was chosen to be 2 h on each side of A and B_3.

Results and discussion

SIM is a fully automated testing method once the yarn is fixed in the clamps. The variation of cross-head movement with time (and the load level, which should be constant) are fed into a computer. From these raw data it is vital to determine the absolute zero strain of the stress versus strain curve, which is taken as the value from Fig. 3, as discussed above.

To illustrate the procedure, one SIM test (SIM70-01-01) is described in detail to show the vertical, rescaling and shifting adjustments used to obtain a smooth master curve.

Figure 8 shows the variation of creep strain with time at pre-defined temperature steps; the strain values have been adjusted so that the initial strain (1.6721%) is the value taken from Fig. 3, and jaw effects have been allowed for, but otherwise this is the raw test data. Figure 9 shows an enlarged view of the first temperature step (25–40 °C); there is some very small variation in strain because the test machine maintains the load by making very small adjustments between very narrow limits. The creep gradients on each side of each temperature step were calculated as described above and tabulated in Table 4.

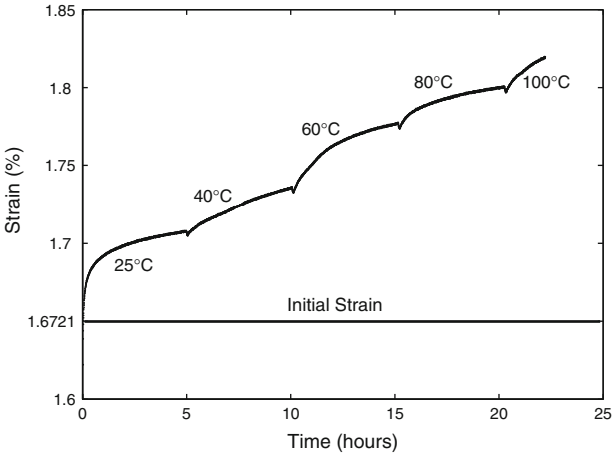

Fig. 8 Strain versus time for test SIM70-01-01

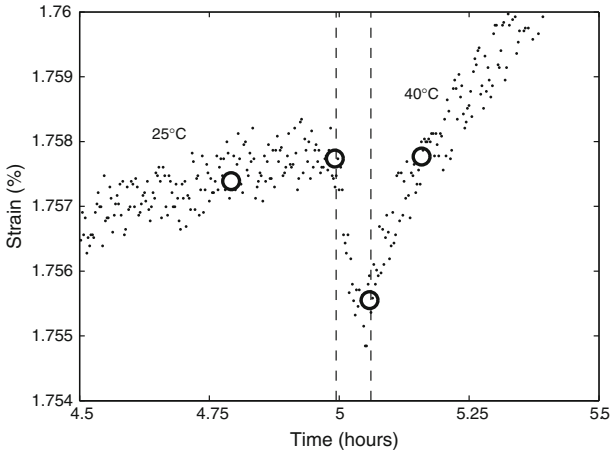

Fig. 9 Detailed strain versus time for first temperature step of test SIM70-01-01

Figure 10 shows the variation of the creep gradient at the temperature step of 25 °C, obtained in preliminary tests from 25 to 40 °C, and from 25 to 60 °C, and the corresponding quadratic which is used with Eq. 8 to determine the vertical shift B′B. Similar calculations were performed at each temperature step; Figure 11 shows the creep data values, as measured, and after the vertical adjustment at each temperature step. The vertical adjustment has eliminated the kinks that occur at each temperature change.

Table 4 Creep gradient values at each temperature step of SIM70-01-01

Test no.	Temperature steps (°C)	Creep gradients (strain/h)	
		Before the temp. step	After the temp. step
SIM70-01-01	25–40	0.0018	0.0171
	40–60	0.0037	0.0301
	60–80	0.0031	0.0245
	80–100	0.0025	0.0259

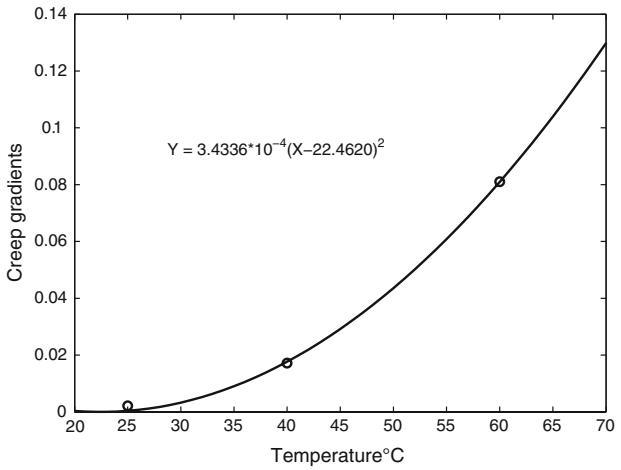

Fig. 10 Creep rates after first temperature step from 25 °C to higher value

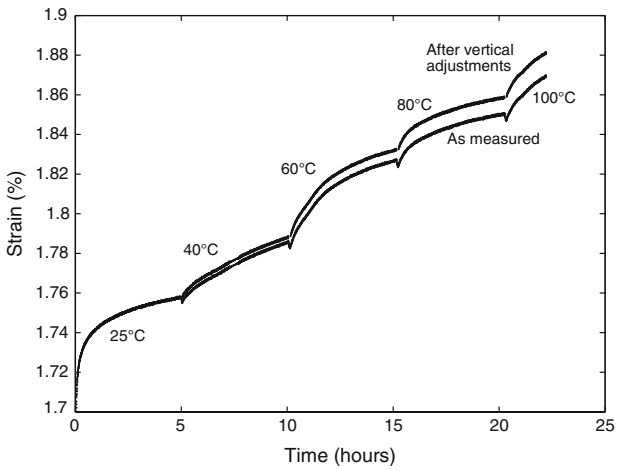

Fig. 11 Test SIM70-01-01 after vertical adjustment

The rescaling and shifting steps are then carried out. Once again, the temperature step from 25 to 40 °C for test SIM70-01-01 is considered in detail. A third-order polynomial was fitted to Eq. 12 and optimised as described above. The optimum rescaling shift was found to be 4.55 h and the horizontal shift was found to be 1.03 decades (on log (time) scale). These values give the fitted curve as

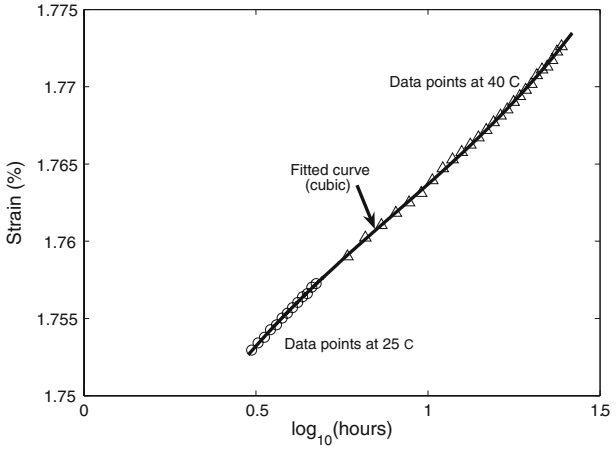

Fig. 12 Third-order polynomial fitted through first temperature step of test SIM70-01-01

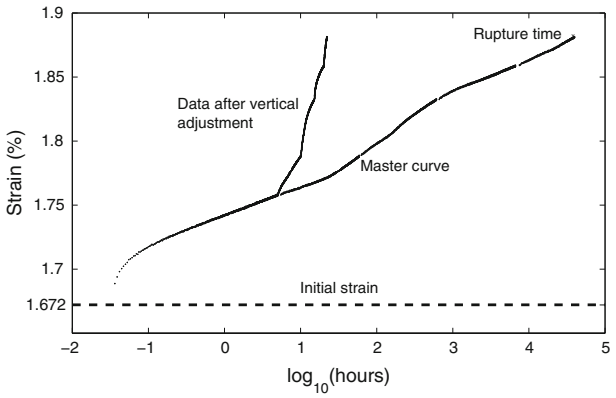

Fig. 13 Master curve for test SIM70-01-01 after all adjustments

shown in Fig. 12. The same process is then repeated at each temperature step, to give the final generated master curve in Fig. 13, which also shows with data after vertical adjustment but before rescaling and shifting.

The same procedure was carried out for all SIM tests at both 50 and 70% ABL.

Validating the SIM method

A series of conventional creep tests have been performed to check the validity of this method [7]. These tests have been carried out in a controlled temperature (25 °C) and humidity (65% RH) level. For comparison, SIM70-01-01 data are plotted in Fig. 14 with the TTSP data [8] and conventional creep data at 70% ABL. Similar results are given in Fig. 15 for tests at 50% ABL. The curves match reasonably closely, but of course the conventional tests are limited by the length of time that was available.

The SIM test picks up the basic form of the results, but the question remains about repeatability. To test this, tests

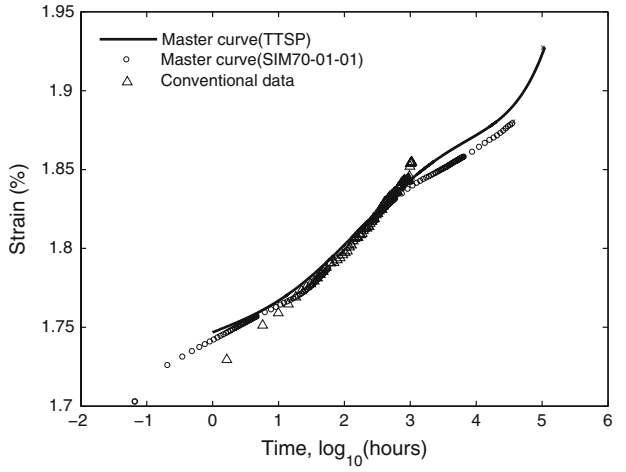

Fig. 14 Comparison between test SIM70-01-01 and other test methods

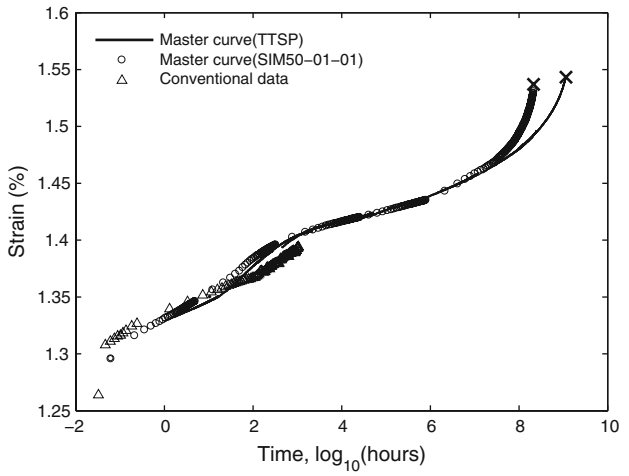

Fig. 15 Comparison between test SIM50-01-01 and other test methods

were carried out with different temperature steps and different durations. Some fibre-to-fibre variation is to be expected, but as shown in Fig. 16 (70% ABL) and Fig. 17 (50% ABL) the SIM curves all match reasonably well in both shape and position. This encourages belief that the method is repeatable.

Chambers [15] and Guimaraes [11] determined the creep capacity of the aramid ropes. Figure 18 shows three regions of the creep curve for a rope. According to Guimaraes' study, the creep capacity is defined as:

$$\varepsilon_2 - \varepsilon_0 \tag{13}$$

where ε_0 is the strain just after the loading. In Chamber's study this is considered as the strain at 1 min just after the initial loading. ε_2 is the strain at the beginning of the tertiary creep state, which is identified as the point where the creep rate starts to accelerate towards failure.

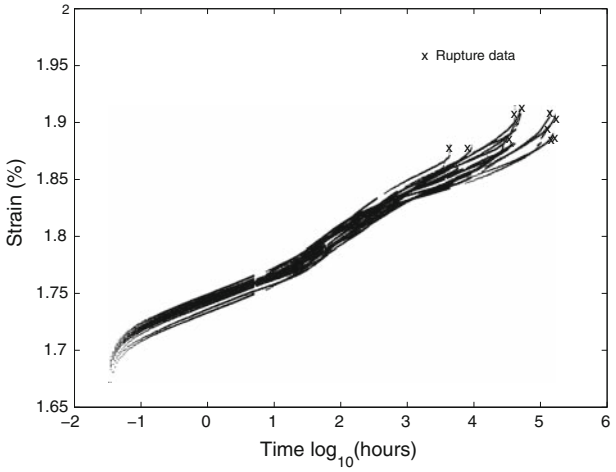

Fig. 16 All master curves for SIM tests at 70% ABL

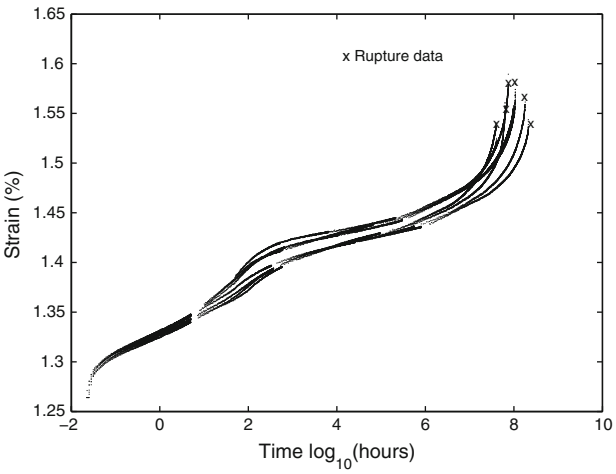

Fig. 17 All master curves for SIM tests at 50% ABL

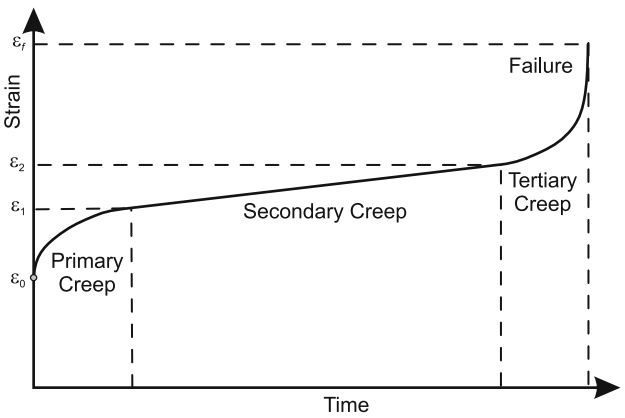

Fig. 18 Generic creep curve

Both Chambers and Guimaraes suggested that aramid fibres might fail when a certain amount of creep capacity had been consumed, and suggested that this effect could be

used to provide experimental predictions of the stress-rupture lifetime if the creep rates could be established.

Figures 16 and 17 do not obviously follow the schematic curve in Fig. 18, but there are notable steep changes at the ends of the SIM master curves, particularly for 50% ABL, which indicates possible tertiary behaviour. The creep capacity has been determined for each SIM curve and tabulated in Table 5, together with Chambers' and Guimaraes' test data. It is apparent that about 0.2% of creep capacity is possible for both stress levels of Kevlar-49 yarns. In contrast, Chambers' data show about 0.14% for 60 tonne ropes and Guimaraes' data show about 0.1% for both 1.5 and 3 tonne ropes. There are difficulties defining the transitions between each creep phase, but the present tests do give some credence to the idea that aramid fibres may fail in stress-rupture when a certain amount of creep strain has taken place.

The initial part of Fig. 14 shows that the SIM master curve matches reasonably well the curve obtained from a conventional creep test, but the master curves as a whole show double curvature between 100 and 10,000 h in all Fig. 14–17. The same behaviour was observed for the master curves generated from TTSP [8]. This reverse creep

Table 5 Creep capacity data for Kevlar ropes and yarns

60 tonne ropes [15]	3 and 1.5 tonne ropes [11]		Kevlar-49 yarns	
$\varepsilon_2 - \varepsilon_0$ (%)	$\varepsilon_2 - \varepsilon_0$ (%)		Specimen no.	$\varepsilon_2 - \varepsilon_0$ (%)
0.10	1.5 tonne	0.116	SIM70-01-01	0.198
0.14		0.096	SIM70-01-02	0.210
0.18		0.110	SIM70-02-01	0.203
0.15		0.092	SIM70-02-02	0.200
0.09		0.111	SIM70-03-01	0.188
0.16		0.118	SIM70-03-02	0.203
0.12		0.106	SIM70-04-01	0.212
0.18	3 tonne	0.108	SIM70-04-02	0.218
–		0.114	SIM70-05-01	0.215
–		0.098	SIM70-05-02	0.218
–		0.097	SIM70-06-01	0.190
–		0.106	SIM70-06-02	0.203
–		0.087	SIM70-07-01	0.187
–		0.071	SIM70-07-02	0.193
–		0.103	SIM70-08-01	0.203
–		0.087	SIM70-08-02	0.207
–		0.116	SIM50-01-01	0.196
–		0.074	SIM50-01-02	0.196
–		0.082	SIM50-02-01	0.191
–		0.106	SIM50-02-02	0.206
–		0.077	SIM50-03-01	0.206
–		0.083	SIM50-03-02	0.201
–	–	–	SIM50-06-01	0.216
–	–	–	SIM50-06-02	0.216

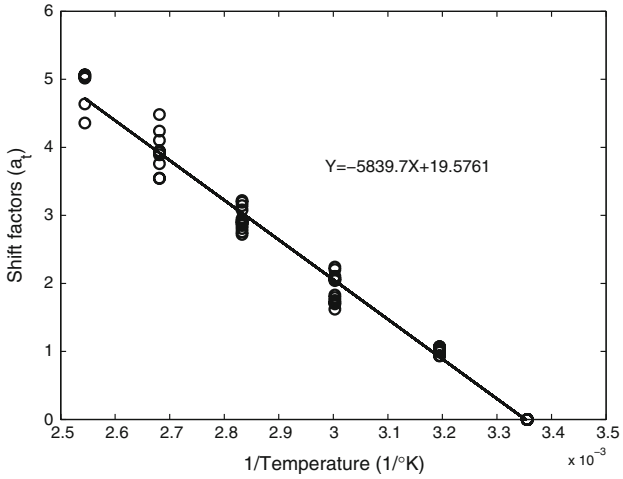

Fig. 19 Arrhenius plot for shift factors for tests at 70% ABL

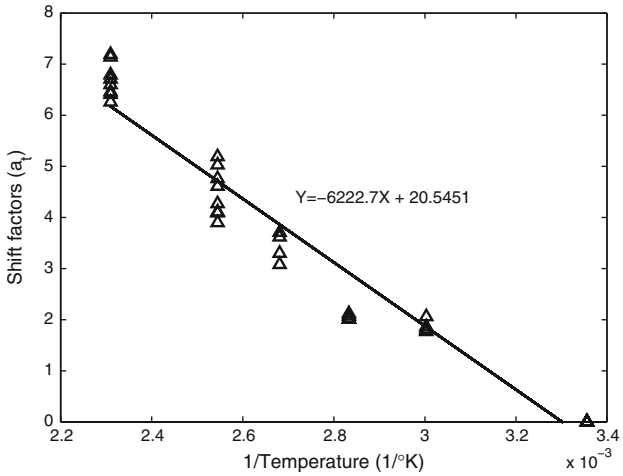

Fig. 20 Arrhenius plot for shift factors for tests at 50% ABL

behaviour has not been described in the literature and this may be the first time it has been observed. It is possible that it may be attributed to some rearrangement of internal structure of the fibres and is independent of the accelerating method. More work should be done to confirm this phenomenon and to suggest a mechanism for it.

As stated in the 'Introduction' section, one of the main assumptions of the method is that the same mechanism should be operative at each temperature level. To check the validity of this phenomenon, all shift factors have been plotted on an Arrhenius plot. Figure 19 shows the SIM data at 70% ABL. The data can be fitted to a line which corresponds to an activation energy of 111.9 kJ/mole. Figure 20 shows the similar plot for the 50% ABL tests, with an activation energy of 119.3 kJ/mole. The fact that the lines are straight, and there are similar activation energies, implies that the same creep mechanism is active at both stress levels and at all temperatures. The creep activation energies obtained from the TTSP [8] were 116.3 and

147.3 kJ/mole at 70 and 50% ABL, respectively. The creep activation energy at 50% ABL from the TTSP is high when compared to the SIM value, but is based on one test, whereas the SIM data values are derived from 8 master curves.

Stress-rupture points

The final stage is to investigate the stress-rupture behaviour. Each of the master curves on Figs. 16 and 17 ends with failure of a yarn. Tables 6 and 7 show the rupture times of SIM tests at 70 and 50% ABL, respectively.

Figure 21 shows stress-rupture test data obtained from aramid ropes, together with extrapolations from the most reliable statistical model fitted to that data [16]. The data from the SIM tests, and also the TTSP tests [8], are shown on the same plot. It is apparent that the failure times of SIM data at 50% ABL are significantly longer than the predictions of the statistical model, while the discrepancy at 70% ABL is much lower. However, most of the rope test data are obtained at much higher load levels, and that data are significantly affected by the relatively short-term tests where the time taken to apply the load may be significant. There is clearly more work that needs to be done to provide more SIM data that extends the values obtained here, and covers also the higher stress levels where there is directly comparable data.

Table 6 Rupture times of SIM curves at 70% ABL

Test number	Rupture times in years
SIM70-01-01	4.5473
SIM70-01-02	5.5580
SIM70-02-01	3.5729
SIM70-02-02	3.0805
SIM70-03-01	0.4007
SIM70-03-02	1.0307
SIM70-04-01	15.5064
SIM70-04-02	18.1984
SIM70-05-01	5.4322
SIM70-05-02	4.5816
SIM70-06-01	1.7770
SIM70-06-02	3.8891
SIM70-07-01	0.6467
SIM70-07-02	0.4873
SIM70-08-01	13.3544
SIM70-08-02	16.9514

Table 7 Rupture times of SIM curves at 50% ABL

Test number	Rupture times in years
SIM50-01-01	24,329
SIM50-01-02	20,434
SIM50-02-01	12,359
SIM50-02-02	11,198
SIM50-03-01	7,226
SIM50-03-02	4,493
SIM50-06-01	4,634
SIM50-06-02	8,550

General discussion of SIM

The SIM approach is an empirical method that can be used to predict the long-term visco-elastic behaviour of polymeric materials with reasonable accuracy. The master curve represents the behaviour at a specific stress and at a specified reference temperature. However, the reliability of the master curve is based on the validity of the assumptions made in the superposing techniques. Parameters such as the rescaling factor, r, and shift factor $\log(a_t)$ need to be determined iteratively, and there is an element of subjectivity in choosing some of the values.

The feasibility of obtaining a smooth master curve depends on the accuracy of the testing technique. Generally yarns are tested in an oven where the temperature can be controlled in a step-wise manner. Since the magnitude of the temperature step is needed as a parameter in generating the results, the oven should be capable of maintaining a constant temperature with a high accuracy. The most important factor is the ability to heat the oven to any desired temperature within a reasonable time to avoid creep recovery. In addition, the same temperature should be maintained over the whole length of the specimen.

Another important factor is the magnitude of the time and temperature steps. Small temperature steps and large time steps would be preferable but take time. To obtain failure of the yarns, large temperature steps were used in the SIM curves at 50% ABL. The differences between the curves can be clearly seen in Fig. 17 in the period between 100 and 10,000 h. There was more variation in the master curves when larger temperature steps were used. If the temperature step is high there is a bigger gap in the master curve at each step (between points A and B_3 in Fig. 1d), which can lead to difficulties in fitting the polynomial across the step. The smaller the gap the less the uncertainty in the shift factors, so it is always advisable to use smaller temperature steps to obtain accurate master curves.

Conclusion

The work described here has shown that the SIM can be readily applied to generate long-term stress-rupture data of

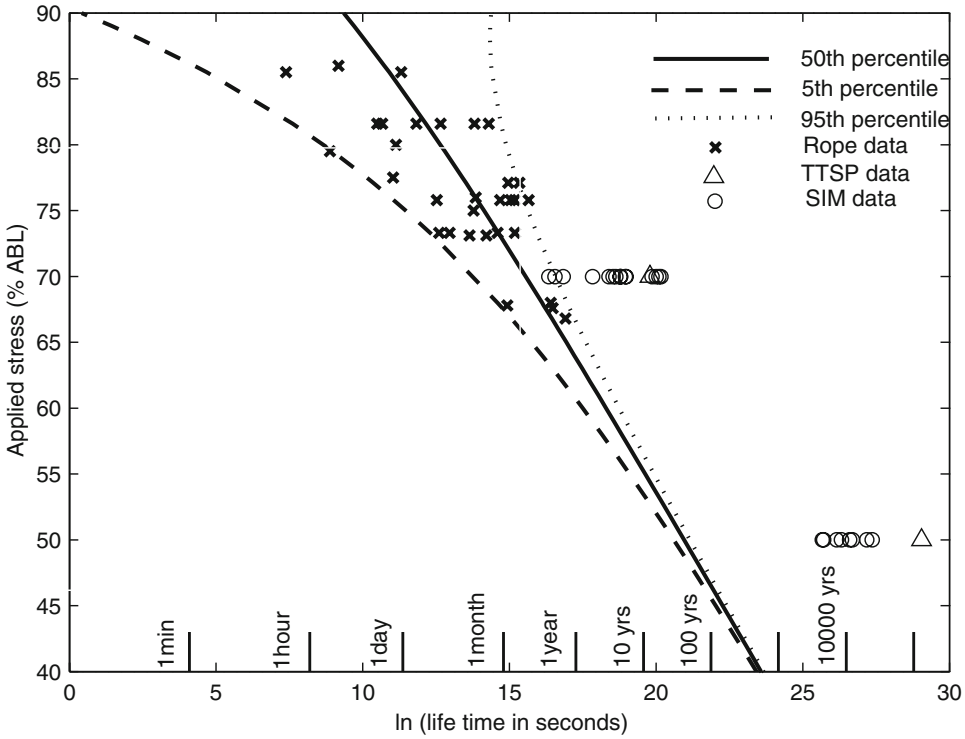

Fig. 21 Stress rupture predictions from SIM testing compared with other test data

aramid yarns and can be used to mimic the behaviour of TTSP tests. The SIM technique has many advantages over conventional TTSP; it is an automated process where a single specimen at each stress level can be tested for the entire thermal history within a reasonably short time scale. The effects of variability of yarns can thus be minimised. However, great care needs to be taken, since a small variation in the testing procedure can have significant effects on the predicted stress rupture lifetime after the various scaling and shifting factors are applied. It is also necessary to carry out many subsidiary tests to determine creep rates during the transitions.

The tests showed that the same creep mechanism was operating at all stress levels and at all temperatures. SIM results showed repeatability, but there was a variation of the rupture times, which may attributed to the variability of the yarns.

Overall, the tests showed that the SIM technique offers (the only) route to the determination of stress rupture lifetime of high-strength, high-stiffness, low-creep materials such as aramids. Such data will be essential for their practical application in many fields in the future.

References

1. Thornton JS, Allen SR, Thomas RW (1997) Approaches for the prediction of long term viscoelastic properties of geosynthetics from short term tests Geosynthetics. IFAI, vol 1. Long Beach, CA, pp 277–291
2. Thornton JS, Allen SR, Thomas RW, Sandri D (1998) The stepped isothermal method for TTS and its application to creep data on polyester yarn. Sixth International Conference on Geosynthetics, Atlanta, USA
3. Thornton JS, Paulson JN, Sandri D (1998a) Conventional and stepped isothermal methods for characterizing long term creep strength of polyester geogrids. Sixth International Conference on Geosynthetics, Atlanta, USA
4. ASTM D6992-03. Standard test method for accelerated tensile creep and creep-rupture of geosynthetic materials based on time-temperature superposition using the stepped isothermal method
5. Zornberg JG, Byler BR, Knudsen JW (2004) J Geotech Geoenviron Eng ASCE 130(11):1158
6. Tamuzs V, Maksimovs R, Modniks J (2001) In: Burgoyne CJ (ed) Fibre reinforced plastics for reinforced concrete structures (FRPRCS-5). Cambridge, UK, p 527
7. Alwis KGNC (2003) Accelerated testing for long-term stress-rupture behaviour of aramid fibres. Thesis submitted to the University of Cambridge
8. Alwis KGNC, Burgoyne CJ (2006) J Appl Compos Mater 13(4):249. doi:10.1007/s10443-006-9017-8
9. Ferry JD (1970) Viscoelastic properties of polymers. Wiley
10. Arridge RGC (1975) Mechanics of polymers. Oxford University Press, London
11. Guimaraes GB (1988) Parallel-lay aramid ropes for use in structural engineering. PhD thesis submitted to the University of London
12. Pottick LA, Allen SR, Farris RJ (1984) J Appl Polym Sci 29:3915. doi:10.1002/app.1984.070291224
13. Ii T, Tashiro K, Kobayashi M, Tadakoro H (1987) Macromolecules 20:347. doi:10.1021/ma00168a020
14. Rojstaczer S, Cohn D, Marom G (1985) J Mater Sci Lett 4:1233. doi:10.1007/BF00723467
15. Chambers JJ (1986) Parallel-lay aramid ropes for use as tendons in prestressed concrete. PhD thesis submitted to the University of London
16. Alwis KGNC, Burgoyne CJ (2005) J Compos Constr 9(2):106. doi:10.1061/(ASCE)1090-0268(2005)9:2(106)